Title

A Drosophila melanogaster Model of Diastolic Dysfunction and Cardiomyopathy Based on Impaired Troponin-T Function

Journal

Circulation Research, 114(2)

ISSN

0009-7330

Authors

Viswanathan, Meera Cozhimuttam
Kaushik, Gaurav
Engler, Adam J
et al.

Publication Date

2014-01-17

DOI

10.1161/circresaha.114.302028

Peer reviewed

Circulation Research
JOURNAL OF THE AMERICAN HEART ASSOCIATION

A *Drosophila Melanogaster* Model of Diastolic Dysfunction and Cardiomyopathy Based on Impaired Troponin-T Function

Meera Cozhimuttam Viswanathan, Gaurav Kaushik, Adam J Engler, William J Lehman and Anthony Cammarato

Circ Res. published online November 12, 2013;
Circulation Research is published by the American Heart Association, 7272 Greenville Avenue, Dallas, TX 75231

Print ISSN: 0009-7330. Online ISSN: 1524-4571

A *Drosophila Melanogaster* Model of Diastolic Dysfunction and Cardiomyopathy Based on Impaired Troponin-T Function

Meera Cozhimuttam Viswanathan[1], Gaurav Kaushik[2], Adam J. Engler[2], William Lehman[3] and Anthony Cammarato[1]

[1]Department of Medicine, The Johns Hopkins University School of Medicine; [2]Department of Bioengineering, University of California, San Diego, and; [3]Department of Physiology and Biophysics, Boston University School of Medicine.

Running title: Mutant TnT-Mediated Diastolic Dysfunction in Flies

Subject codes:
[16] Myocardial cardiomyopathy disease
[130] Animal models of human disease
[137] Cell biology/structural biology
[105] Contractile function

Address correspondence to:
Dr. Anthony Cammarato
Division of Cardiology, Department of Medicine
The Johns Hopkins University School of Medicine
Ross 1050, 720 Rutland Avenue
Baltimore, MD 21205
Tel: 410-955-1807
Fax: 410-502-2558
acammar3@jhmi.edu

In October 2013, the average time from submission to first decision for all original research papers submitted to *Circulation Research* was 12.81 days

DOI: 10.1161/CIRCRESAHA.114.302028

ABSTRACT

***Rationale*:** Regulation of striated muscle contraction is achieved by Ca^{2+}-dependent steric modulation of myosin cross-bridge cycling on actin by the thin filament troponin-tropomyosin complex. Alterations in the complex can induce contractile dysregulation and disease. For example, mutations between or near residues 112-136 of cardiac troponin-T, the crucial N-terminal TnT1 tropomyosin-binding region, cause cardiomyopathy. The *Drosophila up*^{101} Glu/Lys amino acid substitution lies C-terminally adjacent to this phylogenetically conserved sequence.

***Objective*:** Using a highly integrative approach, we sought to determine the molecular trigger of *up*^{101} myofibrillar degeneration, to evaluate contractile performance in the mutant cardiomyocytes, and to examine the effects of the mutation on the entire *Drosophila* heart to elucidate regulatory roles for conserved TnT1 regions and provide possible mechanistic insight into cardiac dysfunction.

***Methods and Results*:** Live video imaging of *Drosophila* cardiac tubes revealed the troponin-T mutation prolongs systole and restricts diastolic dimensions of the heart, due to increased numbers of actively cycling myosin cross-bridges. Elevated resting myocardial stiffness, consistent with *up*^{101} diastolic dysfunction, was confirmed by an atomic force microscopy-based nanoindentation approach. Direct visualization of mutant thin filaments via electron microscopy and three-dimensional reconstruction resolved destabilized tropomyosin positioning and aberrantly exposed myosin binding sites under low Ca^{2+} conditions.

***Conclusions*:** As a result of troponin-tropomyosin dysinhibition, *up*^{101} hearts exhibit cardiac dysfunction and remodeling comparable to that observed during human restrictive cardiomyopathy. Thus, reversal of charged residues about the conserved tropomyosin-binding region of TnT1 may perturb critical intermolecular associations required for proper steric regulation, which likely elicits myopathy in our *Drosophila* model.

Keywords:
Drosophila, steric regulation, tropomyosin, thin filament, myosin, diastolic dysfunction cardiomyopathy, animal model contractile proteins

Nonstandard Abbreviations and Acronyms:

Tn	troponin
Tm	tropomyosin
TnC	troponin-C
TnI	troponin-I
TnT	troponin-T
TnT1	N-terminal fragment of troponin-T
HCM	hypertrophic cardiomyopathy
DCM	dilated cardiomyopathy
RCM	restrictive cardiomyopathy
Cs	Canton-S
up^{101}	*upheld*^{101}
IFM	indirect flight muscle
AH	artificial hemolymph
EGTA	ethylene glycol tetraacetic acid
B-state	blocked state
C-state	closed state
M-state	open-state
CC	conical chamber
AFM	atomic force microscopy

INTRODUCTION

Muscle contraction results from an orchestrated series of molecular events that culminate in transient interactions between myosin-containing thick and actin-containing thin filaments. The high propensity for cyclic ATP-dependent acto-myosin associations indicates that without regulation, muscle would remain in a continuous state of contraction, and hence non-functional. Striated muscle regulation is primarily achieved by Ca^{2+}-dependent modulation of myosin cross-bridge binding on actin by the thin filament troponin-tropomyosin complex.[1-3] The complex consists of an elongated coiled-coil tropomyosin (Tm) dimer that extends along 7 monomers of the long-pitch actin helix and three troponin (Tn) subunits: troponin-C (TnC, the Ca^{2+}-binding subunit), troponin-I (TnI, the inhibitory subunit), and troponin-T (TnT, the Tm-binding subunit). These elements (7 actin monomers, 1 Tn complex, and 1 Tm molecule) comprise "regulatory units", which run continuously in series along thin filaments.

It is generally acknowledged that regulatory units adopt various structural "states" characterized by different Tm positions that govern contraction.[1-5] At rest regulatory units are maintained predominantly in the "blocked (B-) state".[5-7] Here, Tm influenced by TnI (and TnT- see below) inhibits contraction by sterically occluding myosin binding sites on actin. Upon activation, Ca^{2+} binding to TnC promotes a release of TnI-mediated inhibition and the movement of Tm azimuthally from subdomains 1 and 2 and toward subdomains 3 and 4 of F-actin resulting in the "closed (C-) state".[5-7] Initial myosin binding to actin subsequently has allosteric effects on thin filaments such that there is further displacement of Tm and spread of accessible myosin binding sites along regulatory units to establish the "open (M-) state" and promote the cooperative activation of contraction.[4,5,8] Thus, as more cross-bridges are recruited there is a proportional increase in active tension generation and transmission of contractile force. The positional states adopted by Tm appear to represent average locations of the coiled-coil as Tm is thought to oscillate dynamically between the B-, C- and M-states at all Ca^{2+} levels, and it is the average azimuthal location of this equilibrium that actually is controlled by Tn, Ca^{2+} and myosin.[4,9,10]

The TnT subunit of the Tn complex consists of two domains that can be separated by limited proteolysis.[11,12] The C-terminal TnT2 domain binds TnI and TnC. Together they form the globular head, core domain of the Tn complex and act as the Ca^{2+} sensor of the thin filament. The N-terminal TnT1 domain is highly helical, terminates in the head-to-tail Tm-Tm overlap region, enhances the cooperativity of myosin S1 binding to the thin filament, and by binding to Tm increases its affinity for actin.[13-17] Moreover, roles for TnT1 in cardiac myofilament regulation are supported by several findings including a report that describes the N-terminal domain of TnT, in the absence of all other Tn components, inhibits myosin interaction with actin-Tm filaments as a result of the TnT1 tail promoting the B-state.[18] These results suggest the Tn tail may directly contribute to the inhibition of muscle contraction in the absence of Ca^{2+} and plays a critical role in modulating the average position of Tm under different physiological, and potentially pathological, conditions.

TnT is the transducer that links the effects of Ca^{2+} binding interactions of the globular head of Tn to the physical location of Tm along the thin filament. This fundamental property is likely compromised by disease-causing mutations. Alterations in the cardiac TnT (cTnT) gene account for roughly 15% of documented familial hypertrophic cardiomyopathy (HCM)-causing mutations with nearly 70% of these localized to cTnT1 (Fig 1).[19-21] cTnT1 mutations are also linked to dilated (DCM) and restrictive cardiomyopathies (RCM) (Fig 1).[22-26] Many of these mutations have been investigated *in vivo*, *in vitro* and *in silico* and have been shown to result in a wide range of complex molecular and physiological effects.[20,21]

The diverse consequences of cTnT1 mutations correlate with the clinical heterogeneity of the myopathic responses.[20,21] A detailed understanding of such disorders can benefit from model systems that facilitate integrative interrogation of disease pathogenesis from the level of the whole organ down to the

molecular machinery. *Drosophila melanogaster* is a powerful genetic model for investigating the structure and function of striated muscle hierarchically. The indirect flight (IFM) and cardiac muscles of insects are, in fact, comprised of myofibrillar proteins that are highly homologous to those expressed in vertebrates.[27,28] Direct structural evidence indicates that the steric Tn-Tm-based regulatory mechanism of contraction operates in insects.[29] Furthermore, *Drosophila* myofibrillar mutants show disparate cardiomyopathic responses analogous to those observed in humans.[30,31] *Drosophila* has a single TnT gene. Specific constitutively expressed TnT point mutations do not perturb assembly of IFM myofibrils but cause their deterioration within days after utilization.[32,33] The up^{101} amino acid substitution, originally described as Glu88Lys, localizes to the TnT1 domain.[33] The corresponding IFM degenerative syndrome was ascribed to abnormal acto-myosin interactions.[33] Since TnT1 forms crucial Tm associations, modulates the average Tm position along regulatory units and accumulates numerous cardiomyopathy-causing mutations, we tested the hypothesis that the up^{101} amino acid substitution induces cardiomyopathy in flies due to contractile dysinhibition and disrupted steric regulation. Thus, we sought to resolve the initial molecular step that triggers up^{101} IFM myofibrillar degeneration, to evaluate cardiomyocyte contractile performance and to examine the effects of the lesion on the entire *Drosophila* heart in order 1) to ascertain critical regulatory roles for conserved TnT1 regions and 2) to provide a possible mechanistic basis for cardiac dysfunction. We show the up^{101} charge reversal induces cardiomyopathy, prolonged periods of muscle activation and excessive cross-bridge formation even at rest. We demonstrate these changes are associated with altered diastolic dimensions and mechanical properties of the heart and its constituent myocytes, *in vivo*. Direct visualization of up^{101} thin filaments reveals the mutation strongly promotes formation of the C-state in the absence of Ca^{2+}, when a B-state is expected, which likely serves as the initial molecular factor for the cardiac pathology. Similarly, human cardiomyopathy mutations dispersed throughout this conserved region likely disrupt critical TnT1-Tm interactions needed to establish Ca^{2+}-dependent thin filament regulatory states.

METHODS

Fly lines, culture conditions and husbandry.

upheld^{101} (up^{101}) mutant flies, originally recovered from a mutagenesis screen of Canton-S Drosophila[32] were obtained from the Bloomington Drosophila Stock Center at Indiana University. The Canton-S strain served as the wildtype control line.

For up^{101} IFM thin filament isolation, up^{101} *f car*; *b el* Mhc^{12} *cn* double mutants were generated by standard mating procedures. The genetic alteration in the Mhc^{12} strain prevents myosin heavy chain accumulation in the IFM. Thus thick filament assembly and up^{101}-induced IFM degeneration does not occur.[33]

All up^{101} analyses were performed on the hearts and thin filaments of homozygous animals.

Confocal microscopy.

Confocal microscopy was performed as detailed by Alayari et al. (2009)[34] with an Olympus FluoView FV10i Confocal Microscope system at 10x magnification.

Cardiac image analysis of semi-intact Drosophila preparations.

Cardiac tubes of three-week old male and female adult flies (n=40-45) were surgically exposed under oxygenated artificial hemolymph (AH) according to Vogler and Ocorr (2009).[35]

Image analysis of heart contractions was performed using high speed movies of semi-intact *Drosophila* preparations as previously.[31,36] 30 second movies were taken at ~120 frames per second using a

Hamamatsu Orca Flash 2.8 CMOS camera on a Leica DM5000B TL microscope with a 10x (0.30 NA) immersion lens. M-mode kymograms were generated using a MATLAB-based image analysis program.[37] Measurements of cardiac dimensions and contractile dynamics were obtained as output from the MATLAB-based program. Two-way ANOVAs were employed to test if the effects of gender or genotype (or if an interaction exists) for each cardiac parameter were significant. When measured values were not normally distributed data were logarithmically transformed and significance confirmed via two-way ANOVA. Large sample sizes mitigated concern regarding infrequent and mild evidence of variance heterogeneity. Significance was assessed at $p<0.05$.

Imaging of blebbistatin-induced changes in cardiac dimensions.

Beating hearts from three-week old female Canton-S (n=15) and up^{101} (n=20) flies were imaged as described above using a 20x (0.50 NA) immersion objective lens. The hearts were recorded at various focal depths to resolve clear cardiac edges along the length of the tube. After filming, hearts were treated with 100µmol/L blebbistatin (Cayman chemical, Ann Arbor, MI) in AH for ~30 minutes at room temperature. Following complete blebbistatin-induced cessation of beating, cardiac tubes were fixed (8% formaldehyde in 1x PBS) for 20 minutes at 25°C and rinsed three times for 10 minutes in 1x PBS with continuous shaking. The hearts were filmed again post-treatment at various focal depths.

Movies of individual hearts, pre- and post-blebbistatin treatment were opened in HCImage Live software. Diastolic and "blebbistatin-relaxed" diameters were measured at identical longitudinal distances and focal depths, which permitted multiple clear edge views, along the tubes. Three distinct diameter measures were recorded across opposing cardiomyocytes of each heart tube and averaged for each fly. The effect of blebbistatin treatment on cardiac diameters was evaluated using a paired t-test of the means of the matched groups before and after blebbistatin incubation. An unpaired t-test was used to identify significant differences in the cardiac response to blebbistatin between genotypes. Significance was assessed at $p<0.05$.

Nanoindentation by atomic force microscopy (AFM).

Nanoindentation, to determine the transverse stiffness at the cellular seam of the conical chamber, was performed with an Asylum Research MFP-3D Bio Atomic Force Microscope mounted on a Nikon Ti-U fluorescence inverted microscope with a 120pN/nm silicon nitride cantilever pre-mounted with a two µm-radius borosilicate sphere (Novascan Technologies, Ames, IA) as previously described.[38] Prior to indentation, up to three semi-intact heart preparations were immobilized on glass coverslips and submerged in AH. Myogenic contractions were confirmed and then arrested with administration of 10mmol/L EGTA in AH. Eight force curves per conical chamber were obtained from discrete locations at the ventral midline from three-week old female Canton-S (n=14) and up^{101} (n=15) flies. Following indentation in EGTA, hearts were washed with fresh AH and restoration of myogenic contraction was confirmed. Hearts were then incubated in 100µmol/L blebbistatin in AH. Inhibition of contraction was confirmed within 30 minutes of incubation. Indentation was repeated at the same cardiac locations. Following final indentation, blebbistatin was photo-inactivated and resumption of myogenic contraction was visually confirmed to ensure myocardium remained viable. Force-indentation curves were analyzed with automated, custom-written software in MATLAB to calculate myocardial elastic modulus or "stiffness" (E, measured in Pascal; Pa) as described previously.[38] All force curves recorded from each heart tube were averaged for each fly. The effect of blebbistatin treatment on cardiac stiffness was evaluated using a paired t-test of the means of the matched groups before and after incubation. Unpaired t-tests were used to identify significant differences 1) in stiffness between genotypes under each chemical condition and 2) in the cardiac response to blebbistatin among genotypes. Significance was assessed at $p<0.05$.

Electron microscopy and three-dimensional reconstruction.
IFM thin filaments were isolated from the thoraces of up^{101} f car; b el Mhc^{12} cn Drosophila according to Cammarato et al., (2004)[29] with the following modifications: the "chemically skinned" thoraces were rinsed in 25ml of rigor solution and homogenized in 0.5ml of fresh buffer in a glass homogenizer. Homogenates were centrifuged at 16,000g for 60 minutes to sediment particulate material, including trace amounts of non-IFM thin filaments still bound in rigor to thick filaments derived from additional thoracic muscles. 0.3ml of the resultant supernatant, which contained IFM thin filaments, was diluted two to ten-fold with either rigor solution by itself or the buffer with 0.1mmol/L $CaCl_2$ added in excess of the EGTA present, immediately prior to preparation for EM. Thin filaments were negatively stained and imaged as detailed previously.[5,29,39]

Helical reconstruction, which resolves actin monomer structure and Tm strands, but not Tn, was performed on IFM thin filament segments which encompassed four-seven regulatory units from 18 *up^{101}* filaments maintained in EGTA and 14 *up^{101}* filaments maintained in the presence of Ca^{2+} according to standard methods.[5,39,40] The statistical significance of densities in reconstructions was computed from the standard deviations associated with contributing points as previously described.[5,39,41,42]

RESULTS

The homologous Tm binding region of TnT1 is associated with multiple disease mutations.

The strongest association between Tm and Tn involves a C-terminal recognition site of striated muscle Tm and TnT1.[43,44] Likewise, evolutionarily conserved sequences within TnT1 presumably mediate interaction with Tm.[44-46] In particular, multiple sequence alignments identified a highly conserved and highly charged domain corresponding to residues 112–136 of human cTnT1 that likely comprise a critical Tm-binding element (Fig 1).[44] The importance of this TnT1 domain is further underscored by the high number of disease-inducing mutations that reside within and closely flank this region (Fig 1). The *Drosophila up^{101}* TnT glutamic acid to lysine amino acid substitution is located just downstream of this element and likely perturbs TnT1-Tm interactions.

The Drosophila up^{101} TnT mutation alters cardiac morphology.

Adult *Drosophila melanogaster* possess a 1mm long pulsatile heart tube, which is located in the abdomen along the insect's body axis and is composed of a single layer of contractile cardiomyocytes (Fig 2A).[47] The myocytes form bilateral rows that join together through specialized cell junctions to create a simple linear tube that extends down the dorsal body wall.[47,48]

Drosophila cardiac morphology is sensitive to mutation. Alexa594-phalloidin staining of fixed Canton-S *Drosophila* heart tubes revealed typical spiraling myofibrillar arrangements within the cardiomyocytes (Fig 2B and C). The fibers were tightly packed with myofilamentous F-actin. Compared to Canton-S hearts, *up^{101}* TnT1 mutant hearts exhibited an apparent loss of myofilaments as noted by reduced F-actin staining relative to that expressed in the retractors of tergite muscles. The mutant heart tube also appeared substantially narrower than that of the wildtype control. The overall morphological effects of the *up^{101}* mutation on the heart, however, seem less severe than the auto-destructive effects of the lesion on the IFM[33].

The Drosophila up^{101} TnT mutation induces restrictive physiology and diastolic dysfunction.

Beating *Drosophila* heart tubes were imaged to further investigate the pathophysiological effects of the up^{101} TnT1 mutation on live cardiac muscle. M-mode traces, which illustrate the positions of the heart wall edges over time, reveal cardiac dimensions and cardiac contraction dynamics (Fig 3A). up^{101} hearts were characterized by reduced diameters and sustained periods of systole relative to control hearts.

We quantified the effects of altered TnT1 on cardiac dimensions and contractile performance and compared the data to those obtained from Canton-S flies (Fig 3B and Online Table I). Mutant TnT1 expression resulted in significantly reduced diastolic and systolic diameters for both male and female up^{101} relative to control flies. Consistent with ~6% (Canton-S) and 4% (up^{101}) gender-related differences in body size (Online Figure I), female *Drosophila* had significantly larger cardiac diameters relative to male flies. A significant interaction effect was determined between genotype and gender for diastolic and systolic diameter measurements. This suggests the up^{101} mutation differentially perturbs male versus female heart dimensions. The effect of the TnT1 lesion on diastolic diameters was greater than that on systolic diameters, which resulted in a significant decrease in mutant fractional shortening relative to control. The mutation appeared to differentially influence male versus female cardiac shortening (interaction p value<0.0001). Overall up^{101} hearts appeared restricted and unable to adequately relax during diastole.

We additionally evaluated inherent myogenic contractile dynamics using motion analysis software (Fig 3B and Online Table I).[37] The heart period, which is the combined length of time required for a single diastolic and subsequent systolic event of the cardiac cycle, was significantly shorter for up^{101} mutant flies relative to control. Therefore, the mutants display a faster myogenic heart rate. Moreover, a significant interaction effect was determined between genotype and gender, which suggests the TnT1 lesion differentially perturbs the heart rate of males relative to female flies. The up^{101} systolic interval was significantly prolonged relative to that of Canton-S. The degree of prolonged contractile events of the mutant hearts was determined to be gender dependent (interaction p=0.003). Dividing the systolic interval by the heart period demonstrates the extent of time during the cardiac cycle the hearts are contracting. Regardless of gender, the up^{101} TnT1 mutation promoted a significant increase in SI/HP ratio.

Thus, as observed in humans exhibiting restrictive cardiac physiology and diastolic dysfunction, the up^{101} TnT1 mutation seemingly perturbs the ability of the myocardium to reestablish resting diastolic diameters and it prolongs systolic contractile events.

The up^{101} TnT1 mutation reduces cardiac tube diameters during diastole by increasing actively cycling cross-bridges.

Blebbistatin is a small molecule inhibitor of several striated muscle myosins and impedes acto-myosin interaction in cardiac preparations from multiple species.[49,50] Blebbistatin treatment of wildtype *Drosophila* cardiac tubes completely prevented heart wall motion within 15-30 minutes (Fig 4A). Interestingly the diameter across the heart wall in the presence of blebbistatin appeared slightly larger than the maximum diameter across the wall during peak diastole. This implies that in *Drosophila* cardiac muscle not all regulatory units are sterically preventing acto-myosin interactions at diastolic Ca^{2+} levels. To quantify the extent of basal, diastolic shortening wildtype Canton-S fly hearts were filmed before and after incubation with blebbistatin. The average diameter following drug treatment was ~3% greater than that determined during diastole (Fig 4B). This difference was highly significant. These data suggest a small population of residual cross-bridges is actively cycling, generating force, reducing myocyte length and establishing basal mechanical tone in wildtype myocardium during diastole. Interestingly, a paired analysis of up^{101} cardiac diameters during diastole and following blebbistatin treatment revealed a highly significant increase of roughly 13% (Fig 4B). Comparing the change in diameters for each genotype

revealed the response to blebbistatin was significantly greater for *up*^{101} hearts relative to that for control hearts (Fig 4B). These observations are consistent with diastolic dysfunction and restrictive physiology due to excessively dysinhibited cross-bridge cycling, enhanced mechanical tone and incomplete relaxation during diastole for the *up*^{101} TnT mutant hearts relative to control hearts.

The Drosophila up^{101} *TnT mutation enhances myocardial stiffness under low* Ca^{2+}.

To gain direct insight into altered mechanical properties of the mutant hearts during diastole, we exploited the unique geometry of the cardiac tube, in particular the conical chamber, to resolve basal tension differences, *in vivo* at the level of individual cardiomyocytes. The transverse stiffness at the cellular seams of the conical chamber is directly related to the amount of contractile stress exerted by, and transmitted to, the adjoined ends of opposing cardiomyocytes. Nanoindentation at the ventral cell–cell junction, where cytoskeletal elements converge, was performed on each genotype under different chemical conditions (Fig 5A). The transverse stiffness of EGTA-inhibited Canton-S cardiomyocytes within the conical chamber was 2kPa and subsequent incubation in blebbistatin reduced stiffness ~25% (Fig 5B). These data corroborate our optical assessment and provide direct mechanical evidence that, at rest, a small number of unimpeded cross-bridges are actively generating force. The transverse stiffness of EGTA-maintained *up*^{101} fibers was 3.3kPa more than 50% higher than that of EGTA-inhibited control cardiomyocytes (Fig 5B). Addition of blebbistatin significantly reduced *up*^{101} transverse stiffness, which more closely resembled that of blebbistatin-treated control flies. The mechanical response to blebbistatin was significantly greater for *up*^{101} myocytes compared to Canton-S myocytes (Fig 5B). These data are consistent with elevated stress at the ends of the mutant cells at rest due to a larger population of uninhibited actively cycling myosin cross-bridges in *up*^{101} cardiomyocytes relative to that in control.

The Drosophila up^{101} *TnT mutation promotes the C-state even in the absence of* Ca^{2+}.

To directly determine the primary consequence of the *up*^{101} glutamic acid to lysine amino acid substitution and to provide a mechanistic basis for myopathy, we generated three-dimensional reconstructions of purified thin filaments expressing the TnT mutation. Thin filaments were isolated from the IFM of *up*^{101} *Drosophila* and either maintained in EGTA or treated with Ca^{2+} prior to negative staining. Electron micrographs showed that the thin filaments were not obviously different from control filaments and possessed the characteristic double helical array of actin subunits and additionally displayed periodic Tn bulges and elongated Tm strands (not shown).[6,29] Three-dimensional reconstructions of the mutant filaments were determined by helical analysis.[40] Surface views showed that Ca^{2+}-dependent Tm strand movement, typical of control filaments[29], was not a general feature of the mutants (Fig 6A). The majority of IFM thin filaments from *up*^{101} flies revealed Tm strands that contacted subdomains 3 and 4 of successive actin monomers in both the absence and presence of Ca^{2+}. However, 17% of individual Ca^{2+}-free mutant thin filaments differed and exhibited Tm strands that contacted actin monomers along the inner edge of subdomains 1 and 2 of F-actin. When the two sets of Ca^{2+}-free data were combined, the Tm density in helical projection can be seen to contact only the inner domains of actin (Fig 6B). Therefore, Tm is most associated with the inner aspect of the *up*^{101} IFM thin filaments, distal to known myosin binding sites and hence unlikely to sterically prevent contraction. This is likely responsible for the destructive hypercontraction of the IFM and for the excessive residual cross-bridge cycling in relaxed hearts.

DISCUSSION

TnT makes extensive associations with multiple thin filament components including the TnI-TnC binary complex, Tm and actin and therefore is central to thin filament-mediated regulation of striated

muscle contraction. TnT mutations, which predominately localize to the N-terminal TnT1 domain, are frequently associated with a host of myopathic responses (Fig 1). A number of investigative efforts have shown cardiomyopathic cTnT lesions induce a range of complex effects including altered myofilament *in vitro* sliding velocity, disturbed Ca^{2+} sensitivity of force generation, decreased cTnT-Tm affinity, impaired ability to stabilize the Tm overlap, perturbed efficacy of promoting Tm binding to actin, disrupted folding stability and secondary structure of cTnT1 and mutation-specific changes in peptide flexibility, all of which likely contribute to disease pathogenesis.[44,51-55]

Drosophila muscles are also sensitive to TnT alterations. Previously, constitutive TnT1 mutations were shown to drastically disrupt both the structure and function of IFMs within days of adulthood.[33] We speculate that since the up^{101} mutation resides in the N-terminal region of TnT and it induces myosin-dependent IFM degeneration, the lesion likely causes cardiomyopathy in flies due to contractile dysinhibition and perturbed steric regulation.

TnT-binding Tms from vertebrates and invertebrates share a well-conserved amino acid segment believed to be a critical TnT1 recognition site.[43] Similarly, multiple sequence alignments illustrate a high degree of evolutionary conservation among stretches of TnT1 postulated to be critical for Tm associations (Fig 1).[44] Residues 112-136 of human cTnT were found to be 70% homologous across analyzed sequences, which suggests an essential Tm binding role for this element throughout the animal kingdom. This region is highly charged and intermolecular electrostatic associations likely dictate proper function. Importantly, engineered Tn constructs bind tightly to the thin filament only if they contain the entire 112–136 TnT1 domain.[15,17,44,56] The *Drosophila* up^{101} mutation lies just downstream of this region. Introduction of basic charges could disturb conserved interactions *immediately* at the Tm-TnT1 interface that are required for proper steric regulation. Similarly cTnT cardiomyopathy mutations located in and adjacent to this region (Fig 1) are also expected to influence Tm-TnT1 associations. Interestingly, our data illustrate that the up^{101} charge reversal mutation results in a cardiac phenotype reminiscent of human RCM.

The up^{101} amino acid substitution may also promote molecular pathogenesis by potentially altering overall TnT performance, including mutation-driven propagated effects that could influence TnT function at a distance. These effects may involve 1) changes in helical stability of TnT1 and subsequently the flexibility of this region, which could compromise effective interactions with Tm[53]; 2) alterations in local helical electrostatic compaction and consequently distal helical expansion that drives unwinding and flexibility changes at remote distances along TnT[55,57]; and 3) disruptions that possibly propagate through a complex structural pathway to perturb the affinity of cardiac TnC for Ca^{2+}.[58] The latter could potentially contribute to changes in myoflament Ca^{2+} sensitivity, as frequently observed in other models of TnT-based cardiomyopathies.[21,54,58,59]

Regardless of gender, the up^{101} *Drosophila* mutation markedly reduced diastolic volumes and extended systole in mutant relative to control hearts (Fig 3B). These changes are consistent with diastolic dysfunction, a hallmark of HCM and RCM. Diastolic dysfunction is characterized by impaired relaxation, decreased distensibility and increased myocardial stiffness, which can result from excessive acto-myosin interactions.[60,61] Thus, up^{101} *Drosophila* serve as a unique model to investigate the root of these pathological alterations in myocyte properties.

The diameter changes across the *Drosophila* heart, in response to the myosin-specific inhibitor blebbistatin, suggest that diastole in flies is accompanied by a small but significant population of residual, force generating cross-bridges that actively shorten the cardiomyocytes and impact diastolic tone (Fig 4). Detection of cycling myosin cross-bridges at submaximal, diastolic levels of Ca^{2+}, which affect cardiomyocyte mechanical properties, is not unprecedented.[62,63] Although beyond the scope of the current study, these basal acto-myosin associations could bolster the prominent stretch activation response

common to insect muscle and may have important implications in myofilament length dependent activation of cardiomyocytes. Interestingly, specific TnI-inducing RCM and Tm-causing HCM mutations are associated with excessive cross-bridge cycling during diastole.[64,65] These thin filament mutations were shown to reduce basal sarcomere length and elevate diastolic tension of cardiomyocytes. Likewise, the reduced diastolic diameter of up^{101} hearts is due, in part, to excessive, less inhibited force generating acto-myosin interactions that promote enhanced cell shortening relative to control hearts. Application of the myosin inhibitor however did not restore mutant heart diameter to that of blebbistatin-treated control flies (Fig 4B). Thus, additional remodeling events must transpire over the three week pre-analysis period that influence up^{101} myocyte dimensions. Changes in cellular dimensions are consistent with pathological responses and tissue disorganization that accompany cardiac disease. For example, pathological stimuli associated with several cardiomyopathies induce changes in myocyte geometry and shape that help determine contractile function and whole heart morphology.[66]

The myosin-dependent changes in up^{101} cardiac dimensions are accompanied by differences in resting myocardial stiffness. We employed a novel AFM-based technique to resolve *Drosophila* myocardial tension disparities, *in vivo* with single cell resolution (Fig 5A).[38,67] The geometric nature of the cardiac tube allows indentation and transverse stiffness determination from discrete cellular loci in the intact organ with no mechanical artifacts due to myocyte isolation, seeding or plating. By determining the transverse stiffness at cell junctions, we can directly assess the degree of active longitudinal tension generated and transmitted to the connections between the ends of coupled conical chamber myocytes. Thus, we can quantify the relative extent of contractile dysinhibition by comparing the transverse stiffness at the midventral seam from different genotypes before and after incubation with blebbistatin. Control cardiomyocytes showed roughly a 25% drop in transverse stiffness at the midline upon incubation with the myosin inhibitor, consistent with a small number of residual force-generating acto-myosin associations under low Ca^{2+}, diastole-like conditions (Fig 5B). The transverse stiffness of the up^{101} cardiomyocyte junction was over 60% greater than that of control and showed an ~50% decrease following blebbistatin treatment. The large discrepancies in resting transverse stiffness and in response to the myosin-specific inhibitor indicate the TnT1 mutation promotes a greater number of actively cycling, force generating cross-bridges in up^{101} myocytes relative to Canton-S myocytes and these contribute to the diastolic dysfunction observed under relaxing conditions.

TnT is pivotal in modulating the average position of Tm between the B-, C- and M-states along thin filaments.[21] Disease-causing mutations in Tn subunits may lead to changes in the distribution of these states and therefore disrupt regulation of contractile force.[68] To directly assess a mutation-specific redistribution of regulatory states we purified and imaged up^{101} IFM thin filaments. In the complete absence of Ca^{2+}, surface views of three-dimensional reconstructions of up^{101} thin filaments revealed Tm stands, on average, making contact with the inner domains of successive actin monomers along the long pitch helices of the filament (Fig 6). However, a small amount of density could be seen extending from the extreme inner edge of the outer domains of actin to the Tm strands on these filaments (Fig 6A, black arrowheads). This extra density is the result of a small population of up^{101} thin filaments, which in the absence of Ca^{2+} exhibited Tm in the B-state, as seen with wildtype filaments lacking Ca^{2+}.[29] Nonetheless, the vast majority of the up^{101} thin filaments in the absence of Ca^{2+} were shown to be in the C-state. Thus, TnT products of the up^{101} allele may alter the equilibrium of the Tm position at rest such that at any given time the majority of thin filament regulatory units are in the C-state and not the B-state. This is consistent with the mutation disrupting the inherent, and possibly vital, B-state promoting property of the TnT1 tail[18], a property that appears dependent upon a TnT1 subdomain that includes the up^{101} locus. When the up^{101} mutation is expressed *in vivo* and in the presence of thick filaments, excessive cross-bridge cycling would occur in a dysregulated fashion. Over time this could lead to destruction of the IFM and drive restrictive remodeling in the heart.

Analysis of myocytes from several TnT-based cardiomyopathy models has revealed significant alterations in cellular Ca^{2+} handling.[69,70] Moreover, a *Drosophila* TnI mutant, which is characterized by an enlarged cardiac chamber and cardiac contractile dysfunction, displays abnormalities in the cytosolic Ca^{2+} transient as well as changes in transcription of proteins associated with Ca^{2+} handling.[71] Therefore, the up^{101} TnT mutant may similarly exhibit downstream alterations in Ca^{2+} kinetics and homeostasis that potentially contribute to the observed cardiac phenotype. Quantitative polymerase chain reaction analysis was performed to assay possible changes in the Ca^{2+}-handling biosignature of up^{101} relative to Canton-S hearts (Online Figure II).[71] No significant differences were identified between the lines in transcript levels of L-type Ca^{2+} channels, ryanodine receptors, SERCA, Na/Ca exchangers, or in inositol-3-phosphate receptors. Although this assay does not preclude possible post-transcriptional or post-translational modifications that could influence the encoded proteins, nor does it completely rule out all potential adaptive Ca^{2+} responses, the results suggest the cardiac phenotype we observe is primarily due to the direct, Ca^{2+}-independent, C-state promoting effect the up^{101} TnT mutation exerts on thin filaments.

Our integrative data are consistent with a mechanism of diastolic dysfunction and restrictive cardiac pathology based on a fundamental inability of the homozygous, up^{101} TnT1 mutant thin filaments to properly block myosin cross-bridge cycling at rest (Fig 7). Here, a disproportionally large number of up^{101} regulatory units adopt the C-state under low Ca^{2+} conditions. This permits an exceedingly high number of strong stereospecific acto-myosin associations and excessive formation of the M-state that would promote decreased diastolic heart chamber volumes and elevated diastolic myocardial stiffness. Moreover, inordinate myosin binding increases the affinity of Tn for Ca^{2+}.[1,72,73] Thus, fewer mutant regulatory units required to undergo Ca^{2+}-dependent unblocking combined with enhanced Ca^{2+} sensitivity "primes" the system for systole. As a result, for a given Ca^{2+} transient, systole would commence earlier and terminate later, which is consistent with the highly prolonged systolic intervals observed in up^{101} hearts relative to control.

We anticipate similar, however potentially less severe responses in up^{101} heterozygotes. Due to cooperativity of contractile activation and the continuous nature of regulatory units, the effects of the mutation could potentially be transmitted to neighboring, non-mutant regulatory units and thus influence the regulatory status of regions up- and down-stream of the lesion. These propagated effects along the thin filament may also be sufficient to promote myosin cross-bridge cycling, decreased diastolic chamber volumes and elevated diastolic myocardial stiffness, but potentially to a lesser extent than that found in homozygotes due to the presence of some normally functioning, wildtype regulatory units. Thus, as with other models of cardiomyopathy we expect a relationship between the number of mutant up^{101} alleles and phenotype severity.[74-77]

TnT1 is essential for proper transduction of Ca^{2+} signals and modulation of Tm position along regulatory units in striated muscle. Here we examined the effects of the constitutively expressed up^{101} TnT1 mutation at multiple levels in *Drosophila*. We provide the first, direct structural evidence of how a mutation, adjacent to the conserved Tm-binding element of TnT1, perturbs steric regulation, promotes contractile dysinhibition and diastolic dysfunction and drives cardiac remodeling. Our results emphasize the potential significance of Tm-TnT1 electrostatic associations for proper steric regulation throughout the animal kingdom. Numerous indices of up^{101} cardiac function suggest a shift in equilibrium status of thin filament regulatory units to a mutation-induced preponderance of the C-state even at rest. We propose human cardiomyopathy mutations located in and close to the homologous Tm-binding element of TnT1 may also alter the fundamental B-state promoting role of TnT1[18] and thereby activate pathological remodeling cascades. Overall our study indicates that *Drosophila* is a valuable tool for investigating the most proximal, direct effects of thin filament lesions and that flies are an effective and unique model to resolve, at multiple levels, how such mutations perturb the normal distribution of force generating regulatory states and elicit cardiac dysfunction.

ACKNOWLEDGEMENTS
We thank Douglas Deutschman, Ph.D. (San Diego State University) for help with statistical analysis, Georg Vogler, Ph.D. (Sanford Burnham Medical Research Institute) for artwork assistance and Anna Blice-Baum, Ph.D. (Johns Hopkins University) for technical assistance.

SOURCES OF FUNDING
This work was supported by NIH T32HL105373 and American Heart Association 13PRE14410037 (to GK), by NIH R21HL106529 and DP02OD006460 (to AJE), by NIH R37-036153 (to WL), and by American Heart Association 10SDG4180089 and an American Federation for Aging Research Grant (to AC).

Disclosures
None.

REFERENCES

1. Tobacman LS. Thin filament-mediated regulation of cardiac contraction. *Annu Rev Physiol*. 1996;58:447-481
2. Gordon AM, Homsher E, Regnier M. Regulation of contraction in striated muscle. *Physiol Rev*. 2000;80:853-924
3. Lehman W, Craig R. Tropomyosin and the steric mechanism of muscle regulation. *Adv Exp Med Biol*. 2008;644:95-109
4. McKillop DF, Geeves MA. Regulation of the interaction between actin and myosin subfragment 1: Evidence for three states of the thin filament. *Biophys J*. 1993;65:693-701
5. Vibert P, Craig R, Lehman W. Steric-model for activation of muscle thin filaments. *J Mol Biol*. 1997;266:8-14
6. Lehman W, Craig R, Vibert P. Ca^{2+}-induced tropomyosin movement in *Limulus* thin filaments revealed by three-dimensional reconstruction. *Nature*. 1994;368:65-67
7. Lehman W, Vibert P, Uman P, Craig R. Steric-blocking by tropomyosin visualized in relaxed vertebrate muscle thin filaments. *J Mol Biol*. 1995;251:191-196
8. Lehrer SS, Geeves MA. The muscle thin filament as a classical cooperative/allosteric regulatory system. *J Mol Biol*. 1998;277:1081-1089
9. Maytum R, Westerdorf B, Jaquet K, Geeves MA. Differential regulation of the actomyosin interaction by skeletal and cardiac troponin isoforms. *J Biol Chem*. 2003;278:6696-6701
10. Pirani A, Xu C, Hatch V, Craig R, Tobacman LS, Lehman W. Single particle analysis of relaxed and activated muscle thin filaments. *J Mol Biol*. 2005;346:761-772
11. Perry SV. Troponin T: Genetics, properties and function. *J Muscle Res Cell Motil*. 1998;19:575-602
12. Wei B, Jin JP. Troponin T isoforms and posttranscriptional modifications: Evolution, regulation and function. *Arch Biochem Biophys*. 2011;505:144-154
13. Jackson P, Amphlett GW, Perry SV. The primary structure of troponin T and the interaction with tropomyosin. *Biochem J*. 1975;151:85-97
14. Pearlstone JR, Smillie LB. The binding site of skeletal alpha-tropomyosin on troponin-T. *Can J Biochem*. 1977;55:1032-1038
15. Hill LE, Mehegan JP, Butters CA, Tobacman LS. Analysis of troponin-tropomyosin binding to actin. Troponin does not promote interactions between tropomyosin molecules. *J Biol Chem*. 1992;267:16106-16113
16. Schaertl S, Lehrer SS, Geeves MA. Separation and characterization of the two functional regions of troponin involved in muscle thin filament regulation. *Biochemistry*. 1995;34:15890-15894

17. Hinkle A, Goranson A, Butters CA, Tobacman LS. Roles for the troponin tail domain in thin filament assembly and regulation. A deletional study of cardiac troponin T. *J Biol Chem*. 1999;274:7157-7164
18. Tobacman LS, Nihli M, Butters C, Heller M, Hatch V, Craig R, Lehman W, Homsher E. The troponin tail domain promotes a conformational state of the thin filament that suppresses myosin activity. *J Biol Chem*. 2002;277:27636-27642
19. Watkins H, McKenna WJ, Thierfelder L, Suk HJ, Anan R, O'Donoghue A, Spirito P, Matsumori A, Moravec CS, Seidman JG. Mutations in the genes for cardiac troponin T and alpha-tropomyosin in hypertrophic cardiomyopathy. *N Engl J Med*. 1995;332:1058-1064
20. Willott RH, Gomes AV, Chang AN, Parvatiyar MS, Pinto JR, Potter JD. Mutations in troponin that cause HCM, DCM and RCM: What can we learn about thin filament function? *J Mol Cell Cardiol*. 2010;48:882-892
21. Tardiff JC. Thin filament mutations: Developing an integrative approach to a complex disorder. *Circ Res*. 2011;108:765-782
22. Mogensen J, Murphy RT, Shaw T, Bahl A, Redwood C, Watkins H, Burke M, Elliott PM, McKenna WJ. Severe disease expression of cardiac troponin C and T mutations in patients with idiopathic dilated cardiomyopathy. *J Am Coll Cardiol*. 2004;44:2033-2040
23. Stefanelli CB, Rosenthal A, Borisov AB, Ensing GJ, Russell MW. Novel troponin T mutation in familial dilated cardiomyopathy with gender-dependant severity. *Mol Genet Metab*. 2004;83:188-196
24. Peddy SB, Vricella LA, Crosson JE, Oswald GL, Cohn RD, Cameron DE, Valle D, Loeys BL. Infantile restrictive cardiomyopathy resulting from a mutation in the cardiac troponin T gene. *Pediatrics*. 2006;117:1830-1833
25. Menon SC, Michels VV, Pellikka PA, Ballew JD, Karst ML, Herron KJ, Nelson SM, Rodeheffer RJ, Olson TM. Cardiac troponin T mutation in familial cardiomyopathy with variable remodeling and restrictive physiology. *Clin Genet*. 2008;74:445-454
26. Kaski JP, Syrris P, Burch M, Tome-Esteban MT, Fenton M, Christiansen M, Andersen PS, Sebire N, Ashworth M, Deanfield JE, McKenna WJ, Elliott PM. Idiopathic restrictive cardiomyopathy in children is caused by mutations in cardiac sarcomere protein genes. *Heart*. 2008
27. Bernstein SI, O'Donnell PT, Cripps RM. Molecular genetic analysis of muscle development, structure, and function in *Drosophila*. *Int Rev Cytol*. 1993;143:63-152
28. Cammarato A, Ahrens CH, Alayari NN, Qeli E, Rucker J, Reedy MC, Zmasek CM, Gucek M, Cole RN, Van Eyk JE, Bodmer R, O'Rourke B, Bernstein SI, Foster DB. A mighty small heart: The cardiac proteome of adult *Drosophila melanogaster*. *PLoS One*. 2011;6:e18497
29. Cammarato A, Hatch V, Saide J, Craig R, Sparrow JC, Tobacman LS, Lehman W. *Drosophila* muscle regulation characterized by electron microscopy and three-dimensional reconstruction of thin filament mutants. *Biophys J*. 2004;86:1618-1624
30. Wolf MJ, Amrein H, Izatt JA, Choma MA, Reedy MC, Rockman HA. *Drosophila* as a model for the identification of genes causing adult human heart disease. *Proc Natl Acad Sci U S A*. 2006;103:1394-1399
31. Cammarato A, Dambacher CM, Knowles AF, Kronert WA, Bodmer R, Ocorr K, Bernstein SI. Myosin transducer mutations differentially affect motor function, myofibril structure, and the performance of skeletal and cardiac muscles. *Mol Biol Cell*. 2008;19:553-562
32. Homyk T, Jr., Szidonya J, Suzuki DT. Behavioral mutants of *Drosophila melanogaster*. III. Isolation and mapping of mutations by direct visual observations of behavioral phenotypes. *Mol Gen Genet*. 1980;177:553-565
33. Fyrberg E, Fyrberg CC, Beall C, Saville DL. *Drosophila melanogaster* troponin-T mutations engender three distinct syndromes of myofibrillar abnormalities. *J Mol Biol*. 1990;216:657-675
34. Alayari NN, Vogler G, Taghli-Lamallem O, Ocorr K, Bodmer R, Cammarato A. Fluorescent labeling of *Drosophila* heart structures. *J Vis Exp*. 2009
35. Vogler G, Ocorr K. Visualizing the beating heart in *Drosophila*. *J Vis Exp*. 2009

36. Ocorr K, Reeves NL, Wessells RJ, Fink M, Chen HS, Akasaka T, Yasuda S, Metzger JM, Giles W, Posakony JW, Bodmer R. KCNQ potassium channel mutations cause cardiac arrhythmias in *Drosophila* that mimic the effects of aging. *Proc Natl Acad Sci U S A*. 2007;104:3943-3948
37. Fink M, Callol-Massot C, Chu A, Ruiz-Lozano P, Izpisua Belmonte JC, Giles W, Bodmer R, Ocorr K. A new method for detection and quantification of heartbeat parameters in *Drosophila*, zebrafish, and embryonic mouse hearts. *Biotechniques*. 2009;46:101-113
38. Kaushik G, Fuhrmann A, Cammarato A, Engler Adam J. *In situ* mechanical analysis of myofibrillar perturbation and aging on soft, bilayered *Drosophila* myocardium. *Biophysical journal*. 2011;101:2629-2637
39. Vibert P, Craig R, Lehman W. Three-dimensional reconstruction of caldesmon-containing smooth muscle thin filaments. *J Cell Biol*. 1993;123:313-321
40. Owen CH, Morgan DG, DeRosier DJ. Image analysis of helical objects: The Brandeis helical package. *J Struct Biol*. 1996;116:167-175
41. Milligan RA, Flicker PF. Structural relationships of actin, myosin, and tropomyosin revealed by cryo-electron microscopy. *J Cell Biol*. 1987;105:29-39
42. Trachtenberg S, DeRosier DJ. Three-dimensional structure of the frozen-hydrated flagellar filament. The left-handed filament of *Salmonella typhimurium*. *J Mol Biol*. 1987;195:581-601
43. Li Y, Mui S, Brown JH, Strand J, Reshetnikova L, Tobacman LS, Cohen C. The crystal structure of the C-terminal fragment of striated-muscle alpha-tropomyosin reveals a key troponin T recognition site. *Proc Natl Acad Sci U S A*. 2002;99:7378-7383
44. Hinkle A, Tobacman LS. Folding and function of the troponin tail domain. Effects of cardiomyopathic troponin T mutations. *J Biol Chem*. 2003;278:506-513
45. Jin JP, Chong SM. Localization of the two tropomyosin-binding sites of troponin T. *Arch Biochem Biophys*. 2010;500:144-150
46. Manning EP, Guinto PJ, Tardiff JC. Correlation of molecular and functional effects of mutations in cardiac troponin T linked to familial hypertrophic cardiomyopathy: An integrative *in silico*/*in vitro* approach. *J Biol Chem*. 2012;287:14515-14523
47. Miller A. *The internal anatomy and histology of the imago of Drosophila melanogaster*. *Biology of Drosophila*. 1950
48. Rizki TM. The circulatory system and associated cells and tissues. *The genetics and biology of Drosophila*. 1978;2b:397-452
49. Limouze J, Straight AF, Mitchison T, Sellers JR. Specificity of blebbistatin, an inhibitor of myosin II. *J Muscle Res Cell Motil*. 2004;25:337-341
50. Fedorov VV, Lozinsky IT, Sosunov EA, Anyukhovsky EP, Rosen MR, Balke CW, Efimov IR. Application of blebbistatin as an excitation-contraction uncoupler for electrophysiologic study of rat and rabbit hearts. *Heart Rhythm*. 2007;4:619-626
51. Lin D, Bobkova A, Homsher E, Tobacman LS. Altered cardiac troponin T *in vitro* function in the presence of a mutation implicated in familial hypertrophic cardiomyopathy. *J Clin Invest*. 1996;97:2842-2848
52. Morimoto S, Yanaga F, Minakami R, Ohtsuki I. Ca^{2+}-sensitizing effects of the mutations at Ile-79 and Arg-92 of troponin T in hypertrophic cardiomyopathy. *Am J Physiol*. 1998;275:C200-207
53. Palm T, Graboski S, Hitchcock-DeGregori SE, Greenfield NJ. Disease-causing mutations in cardiac troponin T: Identification of a critical tropomyosin-binding region. *Biophys J*. 2001;81:2827-2837
54. Harada K, Potter JD. Familial hypertrophic cardiomyopathy mutations from different functional regions of troponin T result in different effects on the pH and Ca^{2+} sensitivity of cardiac muscle contraction. *J Biol Chem*. 2004;279:14488-14495
55. Ertz-Berger BR, He H, Dowell C, Factor SM, Haim TE, Nunez S, Schwartz SD, Ingwall JS, Tardiff JC. Changes in the chemical and dynamic properties of cardiac troponin T cause discrete cardiomyopathies in transgenic mice. *Proc Natl Acad Sci U S A*. 2005;102:18219-18224

56. Fisher D, Wang G, Tobacman LS. NH2-terminal truncation of skeletal muscle troponin T does not alter the Ca^{2+} sensitivity of thin filament assembly. *J Biol Chem*. 1995;270:25455-25460
57. Guinto PJ, Manning EP, Schwartz SD, Tardiff JC. Computational characterization of mutations in cardiac troponin T known to cause familial hypertrophic cardiomyopathy. *Journal of Theoretical and Computational Chemistry*. 2007;06:413-419
58. Manning EP, Tardiff JC, Schwartz SD. Molecular effects of familial hypertrophic cardiomyopathy-related mutations in the TnT1 domain of cTnT. *J Mol Biol*. 2012;421:54-66
59. Chandra M, Tschirgi ML, Tardiff JC. Increase in tension-dependent ATP consumption induced by cardiac troponin T mutation. *Am J Physiol Heart Circ Physiol*. 2005;289:H2112-2119
60. Kass DA, Bronzwaer JG, Paulus WJ. What mechanisms underlie diastolic dysfunction in heart failure? *Circ Res*. 2004;94:1533-1542
61. Borbely A, Papp Z, Edes I, Paulus WJ. Molecular determinants of heart failure with normal left ventricular ejection fraction. *Pharmacol Rep*. 2009;61:139-145
62. Campbell KS, Patel JR, Moss RL. Cycling cross-bridges increase myocardial stiffness at submaximal levels of Ca^{2+} activation. *Biophys J*. 2003;84:3807-3815
63. King NM, Methawasin M, Nedrud J, Harrell N, Chung CS, Helmes M, Granzier H. Mouse intact cardiac myocyte mechanics: Cross-bridge and titin-based stress in unactivated cells. *J Gen Physiol*. 2011;137:81-91
64. Davis J, Wen H, Edwards T, Metzger JM. Thin filament disinhibition by restrictive cardiomyopathy mutant R193H troponin I induces Ca^{2+}-independent mechanical tone and acute myocyte remodeling. *Circ Res*. 2007;100:1494-1502
65. Bai F, Weis A, Takeda AK, Chase PB, Kawai M. Enhanced active cross-bridges during diastole: Molecular pathogenesis of tropomyosin's HCM mutations. *Biophys J*. 2011;100:1014-1023
66. McCain ML, Parker KK. Mechanotransduction: The role of mechanical stress, myocyte shape, and cytoskeletal architecture on cardiac function. *Pflugers Arch*. 2011;462:89-104
67. Kaushik G, Zambon AC, Fuhrmann A, Bernstein SI, Bodmer R, Engler AJ, Cammarato A. Measuring passive myocardial stiffness in *Drosophila melanogaster* to investigate diastolic dysfunction. *J Cell Mol Med*. 2012;16:1656-1662
68. Chalovich JM. Disease causing mutations of troponin alter regulated actin state distributions. *J Muscle Res Cell Motil*. 2012;33:493-499
69. Haim TE, Dowell C, Diamanti T, Scheuer J, Tardiff JC. Independent FHC-related cardiac troponin T mutations exhibit specific alterations in myocellular contractility and calcium kinetics. *J Mol Cell Cardiol*. 2007;42:1098-1110
70. Guinto PJ, Haim TE, Dowell-Martino CC, Sibinga N, Tardiff JC. Temporal and mutation-specific alterations in Ca^{2+} homeostasis differentially determine the progression of cTnT-related cardiomyopathies in murine models. *Am J Physiol Heart Circ Physiol*. 2009;297:H614-626
71. Lin N, Badie N, Yu L, Abraham D, Cheng H, Bursac N, Rockman HA, Wolf MJ. A method to measure myocardial calcium handling in adult *Drosophila*. *Circ Res*. 2011;108:1306-1315
72. Moss RL, Razumova M, Fitzsimons DP. Myosin crossbridge activation of cardiac thin filaments: Implications for myocardial function in health and disease. *Circ Res*. 2004;94:1290-1300
73. Hinken AC, Solaro RJ. A dominant role of cardiac molecular motors in the intrinsic regulation of ventricular ejection and relaxation. *Physiology (Bethesda)*. 2007;22:73-80
74. Tardiff JC, Hewett TE, Palmer BM, Olsson C, Factor SM, Moore RL, Robbins J, Leinwand LA. Cardiac troponin T mutations result in allele-specific phenotypes in a mouse model for hypertrophic cardiomyopathy. *J Clin Invest*. 1999;104:469-481
75. James J, Zhang Y, Osinska H, Sanbe A, Klevitsky R, Hewett TE, Robbins J. Transgenic modeling of a cardiac troponin I mutation linked to familial hypertrophic cardiomyopathy. *Circ Res*. 2000;87:805-811
76. Du CK, Morimoto S, Nishii K, Minakami R, Ohta M, Tadano N, Lu QW, Wang YY, Zhan DY, Mochizuki M, Kita S, Miwa Y, Takahashi-Yanaga F, Iwamoto T, Ohtsuki I, Sasaguri T. Knock-

in mouse model of dilated cardiomyopathy caused by troponin mutation. *Circ Res*. 2007;101:185-194

77. Ahmad F, Banerjee SK, Lage ML, Huang XN, Smith SH, Saba S, Rager J, Conner DA, Janczewski AM, Tobita K, Tinney JP, Moskowitz IP, Perez-Atayde AR, Keller BB, Mathier MA, Shroff SG, Seidman CE, Seidman JG. The role of cardiac troponin T quantity and function in cardiac development and dilated cardiomyopathy. *PLoS One*. 2008;3:e2642

78. Murakami K, Stewart M, Nozawa K, Tomii K, Kudou N, Igarashi N, Shirakihara Y, Wakatsuki S, Yasunaga T, Wakabayashi T. Structural basis for tropomyosin overlap in thin (actin) filaments and the generation of a molecular swivel by troponin-T. *Proc Natl Acad Sci U S A*. 2008;105:7200-7205

FIGURE LEGENDS

Figure 1. Multiple sequence alignment of TnT1 segments. Clustal Omega multiple sequence alignment of the Tm binding region of TnT1 from various species: *Hs- Homo sapiens*; *Bt- Bos taurus*; *Oa- Ovis aries*; *Rn- Rattus norvegicus*; *Mm- Mus musculus*; *Gg- Gallus gallus*; *Dm- Drosophila melanogaster*. TRT1- slow skeletal TnT isoform; TRT2- cardiac TnT isoform; TRT3- fast skeletal TnT isoform; *Dm* cTRT- upheld isoform K, the predominant isoform identified in the *Drosophila* heart.[28] Residues are shaded based on degree of conservation. An (*) indicates positions that have identical residues, a (:) indicates conservation with strongly similar residues and a (.) indicates weakly similar residues. The loci of human cardiomyopathy-causing mutations are highlighted: (red) hypertrophic, (blue) dilated, (green) restrictive cardiomyopathy mutations. Residues 113-136 of human cTnT1 are highly conserved across analyzed sequences (encompassed by black box), and are believed to be critical for Tm associations throughout the animal kingdom.[44] The *Drosophila* up^{101} residue (E89K of upheld isoform K) is highlighted in yellow and indicated by ↓. For reference, the *Mus musculus* cardiac TnT1 region modeled by Ertz-Berger et al.[55], the purported Tm-binding residues of human fast skeletal TnT as described by Jin and Chong[45] and the chicken fast skeletal TnT1 fragment resolved by Murakami et al.[78] (PDB: 2Z5H) are underlined.

Figure 2. *Drosophila* heart tube morphology is sensitive to the up^{101} TnT1 mutation. A) Illustration depicting the *Drosophila* heart. The cardiac tube consists of a single layer of contractile cardiomyocytes. Inset: the anterior conical chamber (CC) is ~130μm wide and tapers gradually. The cardiomyocytes of the CC exhibit a characteristic rectangular structure similar to vertebrates and are densely populated with parallel bundles of myofibrils that run the length of the cells. They are symmetrically aligned such that the bipolar ends of the myocytes form prominent "seams" along the midventral and middorsal surface.[48] As a result of this arrangement, the junctional seams of cell-cell contact bear the brunt of contractile stress from opposing myocytes. Depending on gender and on genotype, the remainder of wildtype heart tubes are roughly 70μm in diameter. **B)** Alexa594-TRITC phalloidin stained Canton-S (cs) control and **C)** up^{101} mutant heart tubes. Note obvious differences in cardiac diameter. Furthermore, up^{101} hearts exhibited reduced F-actin staining compared to Canton-S hearts as suggested by diminished fluorescence intensity in the cardiomyocytes relative to that in the retractors of tergite muscles (*). Scale bar = 100μm.

Figure 3. up^{101} *Drosophila* display perturbed cardiac dimensions and contractile properties. **A)** M-mode kymograms generated from high speed videos of beating Canton-S (cs) wildtype and up^{101} heart tubes. Vertical arrows delineate diastolic (DD) and systolic (SD) diameters. Horizontal arrows demarcate complete heart periods (HP) and systolic intervals (SI). Relative to Canton-S hearts, up^{101} cardiac tubes displayed reduced diameters and prolonged periods of systole. **B)** Semi-automated optical heartbeat analysis of Canton-S and up^{101} hearts. Regardless of gender, up^{101} *Drosophila* revealed highly significant alterations in several cardiac structural and functional parameters relative to control flies (also see Online Table I). Significant reductions in cardiac dimensions, in fractional shortening and in heart period as well as prolonged systolic intervals were observed in the mutant flies. The genotype and gender effects on cardiac variables were determined by two-way ANOVA. Together, these data suggest the up^{101} TnT mutation induces restrictive cardiac physiology and incomplete diastolic relaxation.

Figure 4. Blebbistatin has differential effects on diameters of control versus up^{101} TnT1 mutant hearts. Beating hearts were treated with 100μmol/L blebbistatin (Bleb) to identify a potential contribution of disproportionate, strong acto-myosin interactions to up^{101}-mediated diastolic dysfunction. **A)** Top: M-Modes generated from an identical region of the same Canton-S (cs) control heart during its cardiac cycle and following blebbistatin-induced relaxation. Note complete, blebbistatin-generated cessation of cardiomyocyte movement and a slight increase in diameter across the heart tube relative to that during diastole. Bottom: Individual frames from movies of Canton-S and up^{101} hearts during peak diastolic and post blebbistatin treatment time points. The cell-lengthening response to blebbistatin appears greater for mutant hearts relative to that of control. **B)** The diameter across discrete locations of Canton-S

hearts increased from 87.9±2.2μm (mean±SEM) during diastole to 90.5±2.1μm post blebbistatin incubation while that for *up*^{101} hearts increased from 51.7±1.6μm to 58.3±1.7μm. A paired t-test revealed these responses were highly significant (****p<0.0001). The average change in diameter for *up*^{101} hearts (6.60±.29μm) was significantly greater (unpaired t-test, ****p<0.0001) than that determined for Canton-S hearts (2.50±.43μm). This is consistent with a greater number of dysinhibited strong acto-myosin associations during diastole, which promote enhanced myocyte shortening for *up*^{101} hearts relative to control.

Figure 5. Excessive cross-bridge cycling increases the transverse stiffness of *up*^{101} cardiomyocytes An atomic force microscopy-based nano-indentation technique was employed to measure basal myocardial stress and to assess residual active cross-bridges, *in vivo*. **A)** Illustration portraying the nano-indentation scheme of *Drosophila* myocardium. Indentations were made at the ventral midline of the heart tubes under 10mmol/L EGTA-relaxed and 100μmol/L blebbistatin-relaxed (Bleb) conditions. Longitudinal stress, derived from active and unimpeded force-generating acto-myosin associations is transmitted to the midventral seam and can be detected as elevated transverse stiffness via nano-indentation. **B)** The stiffness at identical midventral locations of Canton-S (cs) conical chambers decreased from 1.97±.25kPa (mean±SEM) in EGTA to 1.49±.16kPa post blebbistatin incubation while that for *up*^{101} hearts decreased from 3.28±.32kPa to 1.68±.19kPa respectively. A paired t-test revealed these responses were significant for both Canton-S (**p<0.01) and for *up*^{101} (****p<0.0001) cardiomyocytes. Furthermore, the transverse cardiomyocyte stiffness for *up*^{101} hearts in EGTA was significantly greater (unpaired t-test, #p<0.01) than that determined for Canton-S control hearts. The average blebbistatin-induced change in stiffness for *up*^{101} hearts (1.61±.3kPa) was significantly greater (unpaired t-test, **p<0.01) than that for Canton-S hearts (.48±.12kPa). This is consistent with a higher number of basally dysinhibited acto-myosin interactions, which promote increased myocyte transverse stiffness under low Ca^{2+} conditions, in *up*^{101} hearts relative to control.

Figure 6. Three-dimensional reconstructions of *up*^{101} thin filaments reveal perturbed steric regulation. **A)** Surface views of reconstructed *up*^{101} IFM thin filaments showing the position of Tm strands on actin. The four subdomains of a single actin monomer are labeled on the F-actin control reconstruction (subdomains-1 and -2 = outer domain and subdomains-3 and -4 = inner domain of F-actin). Note the presence of helically wound, continuous strands of Tm density (double-headed black arrows) running longitudinally along the *up*^{101} thin filaments that are not seen on the F-actin control. Under both chemical conditions Tm clearly associated with the inner domains (subdomain-3) of successive actin monomers (triple gray arrows) on *up*^{101} thin filaments. In the absence of Ca^{2+} however, the surface view reveals a small amount of extra density extending from Tm (black arrowheads) to the extreme inner edge of the outer domains (subdomain-1). This additional density is due to Tm on 17% of mutant thin filaments within the average structure remaining in the B-state. Under both chemical conditions however, mutant IFM thin filaments were primarily in the C-state with the outer domains of actin exposed. The average phase residuals (±SD), a measurement of the agreement among thin filaments generating reconstructions in each data set (EGTA and Ca^{2+}) were 61.6˚±5.8˚ and 62.0˚±7.8˚ respectively. The average up-down phase residuals, a measure of the filament polarity were 19.4˚±5.1˚ and 20.4˚±8.6˚ respectively, values comparable to those previously reported. The average number of actin subunits per turn of the genetic helix of the IFM thin filaments were 2.155±.007 and 2.156±.008 respectively, consistent with a 28/13 helix. **B)** Helical projections for F-actin and *up*^{101} IFM thin filaments. Helical projections are formed by projecting component densities of the reconstructions down the long-pitch actin helices onto a plane perpendicular to the filament axis. Thus, the projections reveal the axially averaged positions of F-actin and Tm, which appear symmetrical on either side of the filament. The *up*^{101} TnT1 mutation causes Tm to associate primarily with the inner domains of actin (Ai) in the absence of Ca^{2+}. The helical projections revealed no difference in Tm positioning in the absence or presence of Ca^{2+}, and thus steric regulation is disrupted as a result of the mutation. Densities in all maps were shown to be significant over background noise at greater than the 99.95% confidence levels.

Figure 7: Hierarchical modeling of the diastolic effects of the *up*^{101} TnT1 mutation. Diastole is characterized by low levels of free Ca^{2+}. Control thin filament regulatory units are predominantly maintained in the blocked "B"-state (red Tm). Consequently the majority of myosin heads are in an unbound or weakly bound, non-force generating state. However, a small population of cross-bridges, under basal conditions, forms strong stereo-specific force generating associations. These actively cycling cross-bridges generate a finite amount of contractile stress as characterized by elevated transverse stiffness and slightly shortened cardiomyocytes. Incubation with blebbistatin inhibits basal myosin cross-bridge cycling, relieves residual mechanical stress and restores cardiomyocyte length. However, under low Ca^{2+} conditions the *up*^{101} TnT1 mutation appears to aberrantly promote formation of the "C"-state (green Tm). An increase in the proportion of poorly impeded actively cycling cross-bridges stimulates a high degree of resting mechanical tone and excessive cardiomyocyte shortening. Thus, relative to control cardiac tubes, the subsequent myocardial responses of *up*^{101} cardiac tubes to blebbistatin are significantly elevated. These findings suggest diastolic performance in the mutant hearts is likely severely compromised due to contractile dysinhibition and enhanced myocardial stiffness.

Novelty and Significance

What Is Known?

- The N-terminal troponin-T tail promotes a conformational state of the thin filament that inhibits muscle contraction.
- Mutations in and around the highly conserved tropomyosin-binding region of the N-terminal cardiac troponin-T tail result in diverse human cardiomyopathies.
- The *Drosophila melanogaster* glutamic acid to lysine up^{101} troponin-T mutation resides just downstream of the homologous tropomyosin-binding element and results in skeletal muscle degeneration.

What New Information Does This Article Contribute?

- up^{101} *Drosophila* exhibit a cardiac phenotype that is characterized by restrictive physiology and diastolic dysfunction.
- Under relaxing conditions, up^{101} cardiomyocytes appear shorter and stiffer than control cardiomyocytes due to elevated numbers of basally cycling myosin cross-bridges.
- The up^{101} troponin-T mutation disrupts the thin filament conformational state that suppresses myosin activity under low Ca^{2+} conditions.

Troponin-T mutations result in heterogeneous and diverse myopathies and in vivo models of such disorders could facilitate understanding of the underlying pathophysiology. This study describes an integrative approach to characterize the effects of the up^{101} mutation on the *Drosophila* heart. We show how a troponin-T lesion, adjacent to the evolutionarily conserved and highly charged N-terminal tropomyosin-binding element, perturbs muscle regulation, promotes contractile dysinhibition and diastolic dysfunction and drives cardiac remodeling. Our results highlight the potential significance of troponin-T-tropomyosin electrostatic associations for proper contractile regulation. Human cardiomyopathy mutations that localize in, and close to, the well-conserved tropomyosin-binding domain of troponin-T may also alter thin filament regulatory conformational states and thereby contribute to activation of pathological remodeling cascades.

DOI: 10.1161/CIRCRESAHA.114.302028

Figure 1

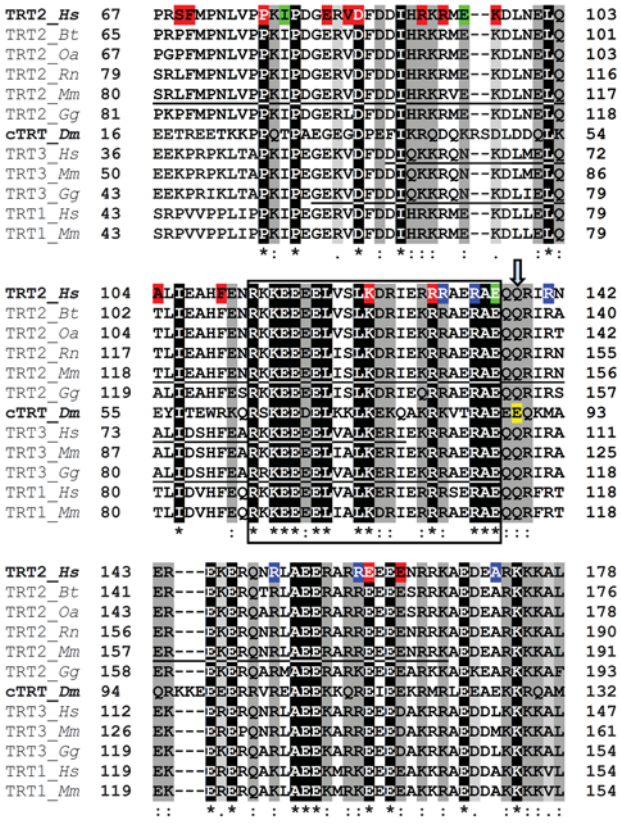

Figure 2

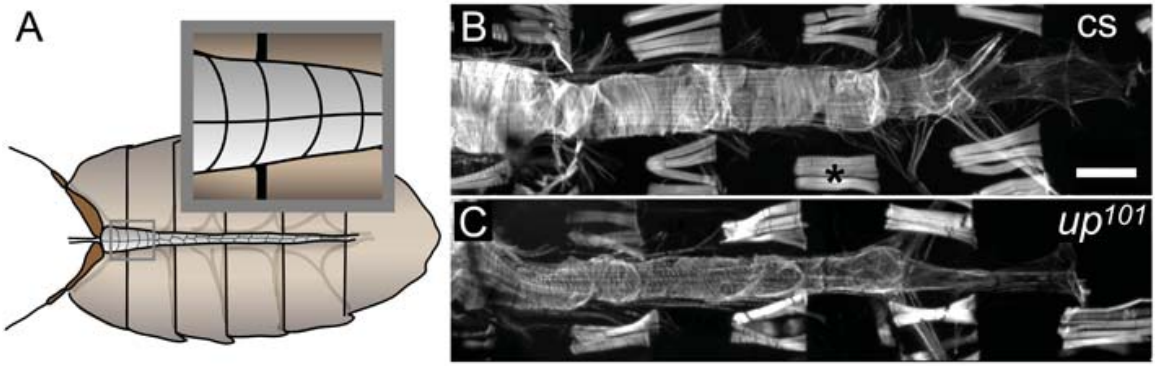

Figure 3

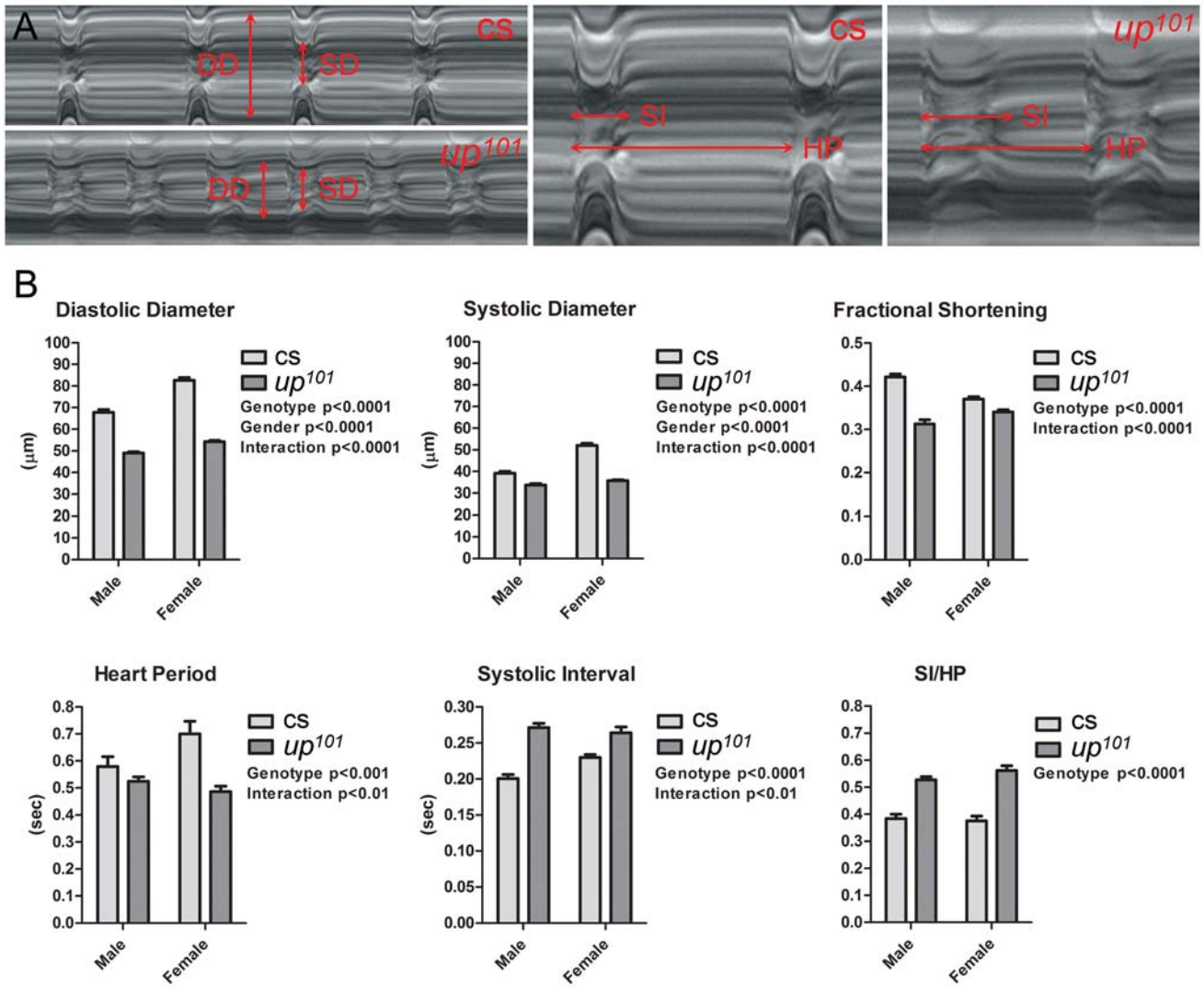

Figure 4

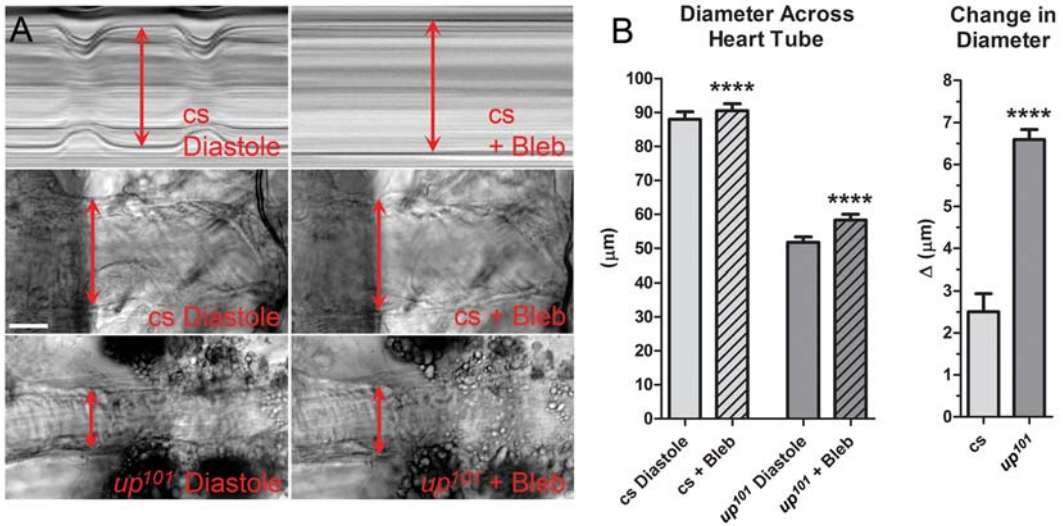

Figure 5

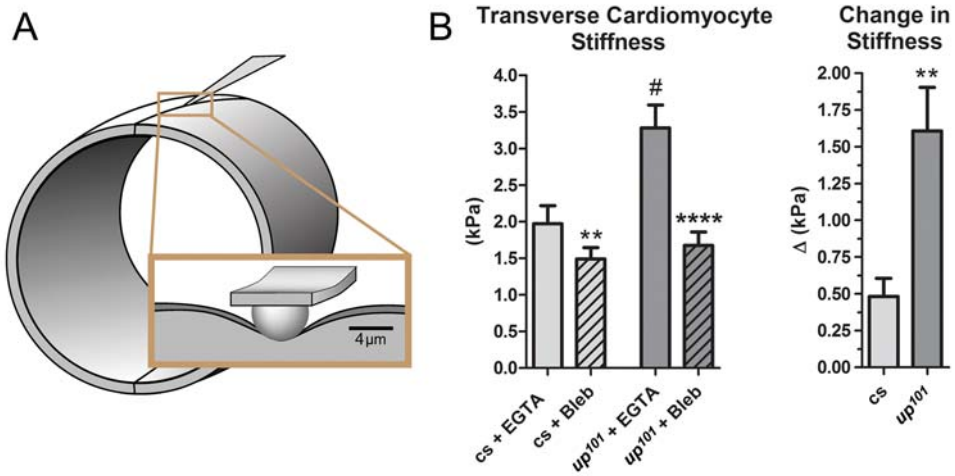

Figure 6

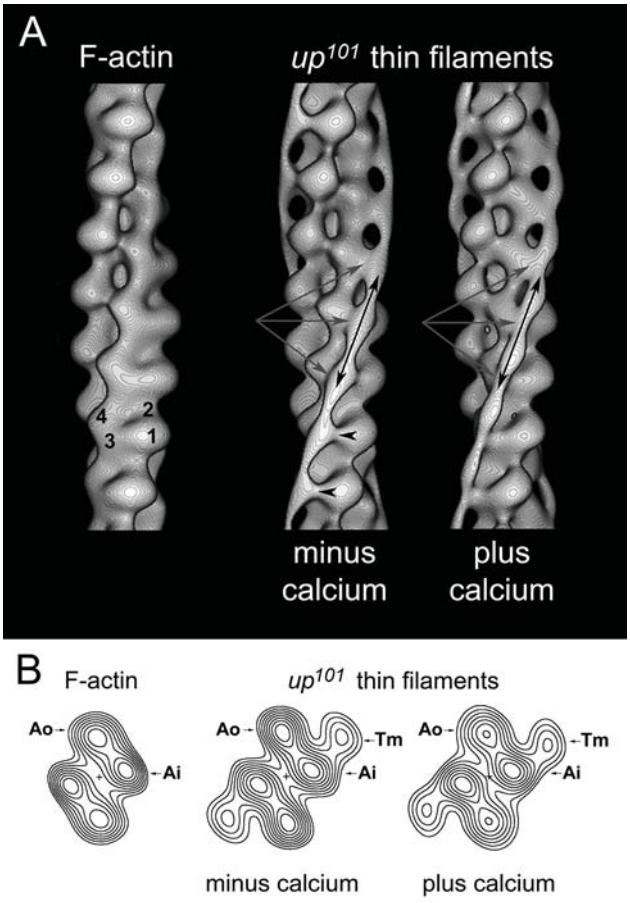

Figure 7

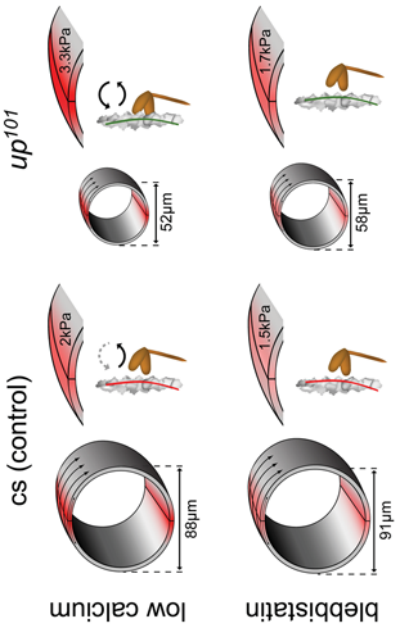

Online Supplemental Methods

Fly lines, culture conditions and husbandry:

upheld^{101} (*up*^{101}) mutant flies, originally recovered from a mutagenesis screen of Canton-S *Drosophila*[1] were obtained from the Bloomington *Drosophila* Stock Center at Indiana University. The Canton-S strain served as the wildtype control line. All *Drosophila* were maintained on a standard yeast-sucrose-agar medium at 25°C. Newly eclosed flies were collected and sexually segregated, over an eight hour span. Flies were transferred to fresh vials every two-three days over a three-week period.

For *up*^{101} IFM thin filament isolation, *up*^{101} *f car*; *b el Mhc*^{12} *cn* double mutants were generated by standard mating procedures. *Mhc*^{12} ''IFM myosinless'' *Drosophila* served as starting material. The genetic alteration in the *Mhc*^{12} strain prevents myosin heavy chain accumulation in the IFM. Thus thick filament assembly and *up*^{101}-induced IFM degeneration does not occur. The *Mhc*^{12} strain has identifiable phenotypic markers, *b*, *el*, and *cn* flanking the myosin gene. These markers were used to follow the *Mhc*^{12} lesion in subsequent crosses. Crosses of *b el Mhc*^{12} *cn Drosophila* with *up*^{101} flies possessing the *f* and *car* markers were carried out to obtain a stable double mutant *up*^{101}; *Mhc*^{12} stock. This stock was used exclusively for native IFM thin filament purification. The filaments are replete with all regulatory components and are thus well-suited for structural and biochemical analyses.[2-5]

Confocal microscopy:

Confocal microscopy was performed as detailed by Alayari et al. (2009).[6] Three-week old female wildtype Canton-S and *up*^{101} *Drosophila* hearts were surgically exposed and arrested using 10mmol/L EGTA in artificial hemolymph. Relaxed hearts were fixed (4% formaldehyde in 1X PBS) and washed thrice with 1X PBST (PBS with 0.1% Triton X-100). Fixed hearts were then stained with Alexa594 TRITC-phalloidin (1:1000 in PBST), rinsed thrice in 1X PBST, mounted and imaged with an Olympus FluoView FV10i Confocal Microscope system at 10x magnification.

Preparation of semi-intact Drosophila *and cardiac image analysis of beating hearts:*

Cardiac tubes of three-week old male and female adult flies (n=40-45) were surgically exposed under oxygenated artificial hemolymph according to Vogler and Ocorr (2009).[7] Briefly, flies were anesthetized and the heads, ventral thoraces, and ventral abdominal cuticles were removed, revealing beating heart tubes. All internal organs and abdominal fat were carefully discarded leaving the heart and associated cardiac tissues.

Image analysis of heart contractions was performed using high speed movies of semi-intact *Drosophila* preparations as previously.[8-11] 30 second movies were taken at ~120 frames per second using a Hamamatsu Orca Flash 2.8 CMOS camera on a Leica DM5000B TL microscope with a 10x immersion lens. M-mode kymograms were generated using a MATLAB-based image analysis program.[10] This provides a trace that documents the movement of the heart tube edges on the y-axis over time on the x-axis.

Measurements of cardiac diameters at peak diastolic and systolic time points were made at two locations along the third abdominal segment of each heart tube, directly from individual movie frames, and averaged together. These individual mean values for all flies of a particular genotype or gender were then used to establish average cardiac diameters. Fractional shortening as well as heart periods and systolic intervals were obtained as output from the MATLAB-based program.[10]

Imaging of blebbistatin-induced changes in cardiac dimensions:

Beating hearts from three-week old female Canton-S (n=15) and *up*^{101} (n=20) flies were imaged as described above using a 20x (0.50 NA) immersion objective lens. The hearts were recorded at various focal depths to resolve clear cardiac edges along the length of the tube. After filming, hearts were treated with 100µmol/L blebbistatin (Cayman chemical, Ann Arbor, MI) in artificial hemolymph for ~30 minutes at room temperature. Following complete blebbistatin-induced cessation of beating, cardiac tubes were fixed (8% formaldehyde in 1x PBS) for 20 minutes at 25°C and rinsed three times for 10 minutes in 1xPBS with continuous shaking. The hearts were filmed again post-treatment at various focal depths.

Movies of individual hearts, pre- and post-blebbistatin treatment were opened in HCImage Live software. Diastolic and "blebbistatin-relaxed" diameters were measured at identical longitudinal distances and focal depths, which permitted multiple clear edge views, along the tubes. Three distinct diameter measures were recorded across opposing cardiomyocytes of each heart tube and averaged for each fly. The effect of blebbistatin treatment on cardiac diameters was evaluated using a paired t-test of the means of the matched groups before and after blebbistatin incubation. An unpaired t-test was used to identify significant differences in the cardiac response to blebbistatin between genotypes. Significance was assessed at $p<0.05$.

Nanoindentation by atomic force microscopy (AFM):

Nanoindentation, to determine the transverse stiffness at the cellular seam of the conical chamber, was performed with an Asylum Research MFP-3D Bio Atomic Force Microscope mounted on a Nikon Ti-U fluorescence inverted microscope with a 120pN/nm silicon nitride cantilever pre-mounted with a two µm-radius borosilicate sphere (Novascan Technologies, Ames, IA) as previously described.[12] Prior to indentation, up to three surgically exposed, beating fly hearts were immobilized on glass coverslips and submerged in freshly oxygenated artificial hemolymph. Myogenic contraction was confirmed and then arrested with administration of 10mmol/L EGTA in hemolymph. Eight force curves per conical chamber were obtained from discrete locations at the ventral midline from three-week old female Canton-S (n=14) and *up*^{101} (n=15) flies. Following indentation in EGTA, hearts were washed with fresh hemolymph and restoration of myogenic contraction was confirmed. Hearts were then incubated in 100µmol/L blebbistatin in hemolymph. Inhibition of contraction was confirmed within 30 minutes of incubation. Indentation was repeated at the same cardiac locations. Following final indentation, blebbistatin was photo-inactivated and resumption of myogenic contraction was visually confirmed to ensure myocardium remained viable. Indentation was performed with an approach and retraction velocity of 1µm/s and <5nN of total load at maximum indentation. No hysteresis or adhesion was observed. Force-indentation curves were analyzed with automated, custom-written software in MATLAB to calculate myocardial elastic modulus or "stiffness" (*E*, measured in Pascal; Pa) as described previously.[12] All force curves recorded from each heart tube were averaged for each fly. The effect of blebbistatin treatment on cardiac stiffness was evaluated using a paired t-test of the means of the matched groups before and after incubation. Unpaired t-tests were used to identify significant differences 1) in stiffness between genotypes under each chemical condition and 2) in the cardiac response to blebbistatin among genotypes. Significance was assessed at $p<0.05$.

Electron microscopy and three-dimensional reconstruction:

IFM thin filaments were isolated from the thoraces of *up*^{101} *f car; b el Mhc*^{12} *cn Drosophila* according to Cammarato et al., (2004)[2] with modifications. 5µl of IFM thin filament suspension in either EGTA or Ca^{2+}-containing rigor buffer was applied to carbon coated EM grids (at ~25°C), negatively stained and rinsed with 1% (w/v) uranyl acetate, and dried at 80% relative humidity to aid in spreading the stain.[13,14] EM images were recorded at 80kV on a Philips CM120 EM at 60,000X magnification under low dose conditions (~12e-/Å) at a defocus of 0.5µm.

Micrographs were digitized using a Zeiss SCAI scanner at a pixel size corresponding to 0.7nm in the filaments, and well-preserved regions of the filaments were selected and straightened as previously.[13,14] Helical reconstruction, which resolves actin monomer structure and Tm strands, but not troponin, was performed on IFM thin filament segments which encompassed four-seven regulatory units from 18 *up*^{101} filaments maintained in EGTA and from 14 *up*^{101} filaments maintained in the presence of Ca^{2+} according to standard methods.[13-15] Thus, structural information from roughly 80 *up*^{101} regulatory units was included in each of the final reconstructions. The statistical significance of densities in reconstructions was computed from the standard deviations associated with contributing points as previously described.[13,14,16,17] Note subtle differences in appearance of overall Tm density and in actin substructure can be introduced as a result of staining inconsistencies as well as from the inclusion of distinct B- and C-state subpopulations of filaments in an average three-dimensional reconstruction.

Quantitative polymerase chain reaction (qPCR):

Total RNA was isolated from dissected hearts of 3 week old flies using the Quick-RNA microprep kit (Zymo Research Corp., Irvine, CA). Contaminating DNA was removed with RNase free DNase I (Qiagen Inc, Valencia, CA). Reverse transcription polymerase chain reactions were performed using Qiagen QuantiTect Reverse Transcription Kits (Qiagen Inc, Valencia, CA) and 10ng of RNA per reaction. Quantitative (Real Time) polymerase chain reactions were carried out on a Bio-Rad CFX96 Touch Real-Time PCR Detection System (Bio-Rad Laboratories Inc.; Hercules, CA). Sequence-specific forward and reverse primers targeting universally-transcribed regions of genes of interest were custom-designed (Integrated DNA Technologies; San Diego, CA). The calcium-handling protein-encoding genes assayed were: Ca-α1D, Rya-44F, Ca-P60A, CalX, Itp-r83A (see gene info and primer list in table below).The following components were used per reaction: 1µL (1-2µg/µL starting concentration) cDNA, 12.5µL 2X Power SYBR Green PCR Master Mix (Life Technologies; Carlsbad, CA), 2.5µL (100µmol/L starting concentration) Forward Primer, 2.5µL (100µmol/L starting concentration) Reverse Primer, and 6.5µL DEPC water for a final reaction volume of 25µL. Reactions with 1µL DNAase/RNAase-free water in lieu of 1µL cDNA in 25µL reaction volume served as negative controls for each gene. The following reaction conditions were used: 10 min at 95°C followed by 40 cycles of a) 95°C for 15 sec and b) 60°C for 60 sec. Starting-quantity of each reaction was calculated by comparing Ct to a standard curve generated from known concentrations of human Fibronectin 1 cDNA and then subtracting negative-control quantity. Each replicate was then normalized to Rpl32 quantity. Finally, we report fold-change as the final average *up*^{101} quantity for a given gene normalized to final average Canton-S quantity. Six independent experiments were performed per gene in duplicate using pools of 12 different hearts per reaction.

qPCR Primers:

	Forward Primer (5'-3')	Reverse Primer (5'-3')
L-type Calcium Channel (Ca-α1D; CG4894; NCBI ID# 34950)	CAACAGCAACAGAGAGAGAGAG	GAACTCGGAGTCGCAGTATTT
Ryanodine Receptor (Rya-44F; CG10844; NCBI ID# 49090)	AAGTGGACTGGTGGCTTTATC	GTTTCTCCTCGTGCTCCATATC
SERCA (Ca-P60A; CG3725; NCBI ID# 49297)	GCCACTGAACGAAGAGGATAA	GACGGCGATCTTGAAGTAGTAG
NCX (CalX; CG5685; NCBI ID# 42481)	CTCAAAGTCCAGGAGACAGAAG	CCCACAAACAGGTAGATCAGTAG
IP3 Receptor (Itp-r83A; CG1063; NCBI ID# 40664)	CTTCTTCCTCCTCACCGTATTC	CACCACAGCTCGTCCATATT
Housekeeper (Rpl32; CG7939; NCBI ID# 43573)	CCAAGGGTATCGACAACAGAG	GTGTATTCCGACCACGTTACA
Standard (Fibronectin 1; NCBI ID# 2335)	AGGCTTGAACCAACCTACGGA	GCCTAAGCACTGGCACAACAG

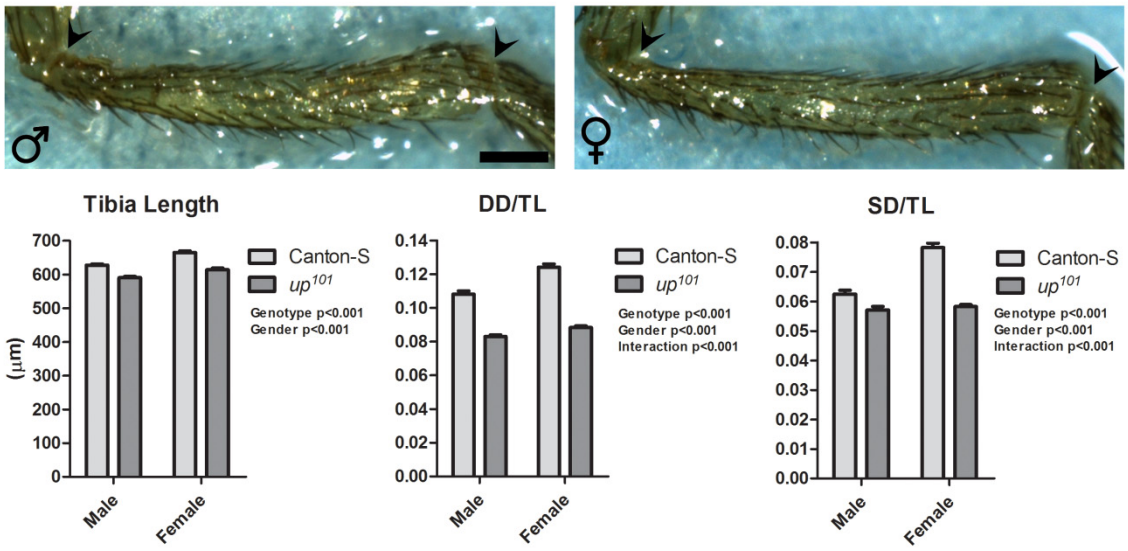

Online Figure I: The contribution of gender and genotype to *Drosophila* body and heart size. Top) The legs of *Drosophila* consist of 9 segments separated by flexible joints. Average tibia contour length was used as an index of body size. We carefully measured tibia length from the flanking joints (arrow heads) of the right middle leg of over 35 Canton-S and up^{101} male and female flies. Scale bar = 100μm. **Bottom)** Average tibia length for female flies was significantly greater than that determined for males while average Canton-S tibia length was significantly greater than that for up^{101}. Thus, both gender and genotype significantly influence *Drosophila* body size. The genotype and gender effects on tibia length were determined by two-way

ANOVA. However, normalizing diastolic (DD) and systolic (SD) cardiac diameters to average tibia length (TL) prior to two-way ANOVA illustrates differences in body size have little influence on the effects of gender and genotype on cardiac diameters.

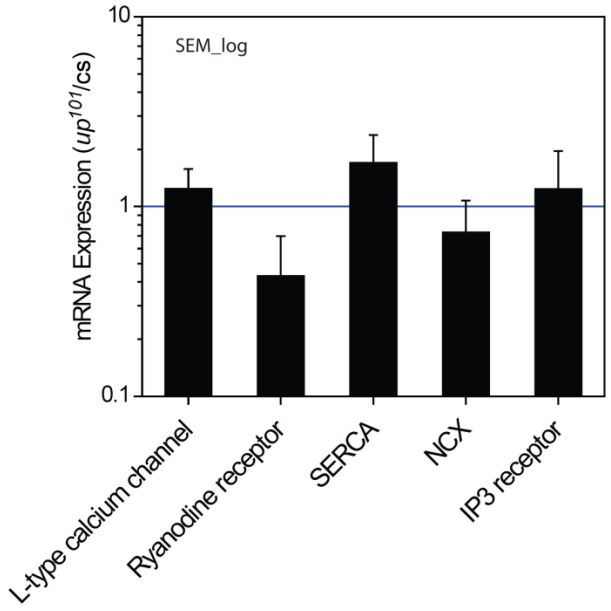

Online Figure II: The *up*^{101} TnT mutation does not influence Ca^{2+}-handling gene expression. Quantitative polymerase chain reaction measurements of transcript expression levels in hearts of *up*^{101} relative to Canton-S flies for L-type Ca^{2+} channels, ryanodine receptors, sarco/endoplasmic reticulum Ca^{2+}-ATPase, Na/Ca exchangers and inositol-3-phosphate receptors. Each replicate was normalized to Rpl32 quantity. Six independent experiments were performed per gene in duplicate using pools of 12 different hearts per reaction. Independent unpaired t-tests of normalized values for each gene revealed no significant differences in the expression of Ca^{2+}-handling genes between Canton-S control and *up*^{101} mutant hearts.

	Canton-S Male ***n*=41** (Mean ± SEM)	***up*^{101} Male** ***n*=41** (Mean ± SEM)	**Canton-S Female** ***n*=45** (Mean ± SEM)	***up*^{101} Female** ***n*=44** (Mean ± SEM)
Heart period (sec)	0.58 ± 0.037	0.53 ± 0.016	0.70 ± 0.047	0.49 ± .0200
Systolic interval (sec)	0.20 ± 0.004	0.27 ± 0.006	0.23 ± 0.004	0.26 ± 0.008
SI/HP	0.38 ± 0.016	0.53 ± 0.011	0.38 ± 0.018	0.56 ± 0.018
Diastolic diameter (μm)	67.88 ± 1.208	49.01 ± 0.588	82.62 ± 1.300	54.29 ± 0.592
Systolic diameter (μm)	39.24 ± 0.808	33.71 ± 0.700	52.08 ± 0.995	35.77 ± 0.426
Fractional shortening	0.42 ± 0.007	0.31 ± 0.009	0.37 ± 0.006	0.34 ± 0.005

Online Table I: The effects of the *up*^{101} TnT mutation on the *Drosophila* heart. Two-way ANOVA results for Online Table I can be found in Fig 3B.

Supplemental References:

1. Homyk T, Jr., Szidonya J, Suzuki DT. Behavioral mutants of *Drosophila melanogaster*. III. Isolation and mapping of mutations by direct visual observations of behavioral phenotypes. *Mol Gen Genet*. 1980;177:553-565
2. Cammarato A, Hatch V, Saide J, Craig R, Sparrow JC, Tobacman LS, Lehman W. *Drosophila* muscle regulation characterized by electron microscopy and three-dimensional reconstruction of thin filament mutants. *Biophys J*. 2004;86:1618-1624
3. Cammarato A, Craig R, Sparrow JC, Lehman W. E93K charge reversal on actin perturbs steric regulation of thin filaments. *J Mol Biol*. 2005;347:889-894
4. Cammarato A, Craig R, Lehman W. Electron microscopy and three-dimensional reconstruction of native thin filaments reveal species-specific differences in regulatory strand densities. *Biochem Biophys Res Commun*. 2010;391:193-197
5. Vikhorev PG, Vikhoreva NN, Cammarato A, Sparrow JC. *In vitro* motility of native thin filaments from *Drosophila* indirect flight muscles reveals that the *held-up 2* TnI mutation affects calcium activation. *J Muscle Res Cell Motil*. 2010;31:171-179
6. Alayari NN, Vogler G, Taghli-Lamallem O, Ocorr K, Bodmer R, Cammarato A. Fluorescent labeling of *Drosophila* heart structures. *J Vis Exp*. 2009
7. Vogler G, Ocorr K. Visualizing the beating heart in *Drosophila*. *J Vis Exp*. 2009
8. Ocorr K, Reeves NL, Wessells RJ, Fink M, Chen HS, Akasaka T, Yasuda S, Metzger JM, Giles W, Posakony JW, Bodmer R. KCNQ potassium channel mutations cause cardiac arrhythmias in *Drosophila* that mimic the effects of aging. *Proc Natl Acad Sci U S A*. 2007;104:3943-3948
9. Cammarato A, Dambacher CM, Knowles AF, Kronert WA, Bodmer R, Ocorr K, Bernstein SI. Myosin transducer mutations differentially affect motor function, myofibril structure, and the performance of skeletal and cardiac muscles. *Mol Biol Cell*. 2008;19:553-562
10. Fink M, Callol-Massot C, Chu A, Ruiz-Lozano P, Izpisua Belmonte JC, Giles W, Bodmer R, Ocorr K. A new method for detection and quantification of heartbeat parameters in *Drosophila*, zebrafish, and embryonic mouse hearts. *Biotechniques*. 2009;46:101-113
11. Ocorr K, Fink M, Cammarato A, Bernstein S, Bodmer R. Semi-automated optical heartbeat analysis of small hearts. *J Vis Exp*. 2009
12. Kaushik G, Fuhrmann A, Cammarato A, Engler Adam J. *In situ* mechanical analysis of myofibrillar perturbation and aging on soft, bilayered *Drosophila* myocardium. *Biophysical journal*. 2011;101:2629-2637
13. Vibert P, Craig R, Lehman W. Three-dimensional reconstruction of caldesmon-containing smooth muscle thin filaments. *J Cell Biol*. 1993;123:313-321
14. Vibert P, Craig R, Lehman W. Steric-model for activation of muscle thin filaments. *J Mol Biol*. 1997;266:8-14
15. Owen CH, Morgan DG, DeRosier DJ. Image analysis of helical objects: The Brandeis helical package. *J Struct Biol*. 1996;116:167-175
16. Milligan RA, Flicker PF. Structural relationships of actin, myosin, and tropomyosin revealed by cryo-electron microscopy. *J Cell Biol*. 1987;105:29-39
17. Trachtenberg S, DeRosier DJ. Three-dimensional structure of the frozen-hydrated flagellar filament. The left-handed filament of *Salmonella typhimurium*. *J Mol Biol*. 1987;195:581-601